PLASMA ROTATION INDUCED BY RF

by
V.S. CHAN, S.C. CHIU, Y.R. LIN-LIU,
and Y.A. OMELCHENKO

MAY 1999

PLASMA ROTATION INDUCED BY RF

by

**V.S. CHAN, S.C. CHIU, Y.R. LIN-LIU,
and Y.A. OMELCHENKO**

**GENERAL ATOMICS PROJECT 3726
MAY 1999**

Plasma Rotation Induced by RF

V.S. Chan, S.C. Chiu,* Y.R. Lin-Liu, and Y.A. Omelchenko

General Atomics, P.O. Box 85608, San Diego, California 92186-5698
*Sunrise R&M, San Diego, California 92129

Abstract. Plasma rotation has many beneficial effects on tokamak operation including stabilization of MHD and microturbulence to improve the beta limit and confinement. Contrary to present-day tokamaks, neutral beams may not be effective in driving rotation in fusion reactors; hence the investigation of radiofrequency (RF) induced plasma rotation is of great interest and potential importance. This paper reviews the experimental results of RF induced rotation and possible physical mechanisms, suggested by theories, to explain the observations. This subject is only in the infancy of its research and many challenging issues remained to be understood and resolved.

1. INTRODUCTION

Plasma rotation has been the subject of intense study in recent years because of its many beneficial effects on tokamak operation. Toroidal rotation in tokamaks has been demonstrated to be necessary for stabilization of magnetohydrodynamic (MHD) modes in order to sustain high beta equilibria [1]. Radial electric field shear generated by sheared rotation, either toroidally or poloidally, has been shown to suppress turbulence and allow improvement in energy confinement [2]. In present-day tokamaks, rotation is mostly driven by unbalanced neutral beam injection (NBI), which may not be effective in the reactor regime. Hence, experimental and theoretical investigation of radio frequency (RF)- induced plasma rotation is of great interest and can potentially be a very important tool for advanced tokamak operation.

A variety of RF effects on toroidal rotation have been reported from tokamak experiments worldwide. In dominantly neutral beam (NBI)-heated discharges, addition of RF heating usually reduces toroidal rotation in the direction parallel to plasma current (co-current rotation), and this has been observed on TFTR, JET, and DIII–D [3–5]. In the case of purely ion cyclotron resonance frequency (ICRF)-heated plasmas, counter-current rotation generated through a RF-induced ion orbit loss mechanism was reported in an early TFTR experiment [6]. On the other hand, co-current rotation has been observed in H–mode discharges with ICRF heating alone on JET and C-Mod [7,8]. While the co-current rotation observed in the JET experiment appears to be correlated with an increasing ion pressure gradient associated with the L–H transition, significant core rotation observed on C-Mod cannot be accounted for by this explanation. Experimental evidence on RF-induced poloidal rotation is less readily available.

Localized sheared poloidal flow generation has been observed in ion Bernstein wave (IBW) heated discharges on PBX-M and TFTR [9,10].

Theoretical explanations of RF-induced rotation can be categorized under different ways of breaking the toroidal symmetry in particle and wave momentum space. Direct momentum input from waves and the presence of loss cones are examples [11,12]. Another promising physical mechanism for understanding the diverse phenomena is non-ambipolar RF induced radial transport of minority or beam ions [13,14], which gives rise to a radial current and $J \times B$ torque for both toroidal and poloidal acceleration. Large drift-orbits and momentum dissipation mechanisms including a non-slip wall play significant roles in these theoretical models.

The organization of the paper is as follows. A review of experimental results is presented in Section 2. Section 3 discusses theoretical models of RF induced rotation, beginning with a discussion of the toroidal and poloidal flow equations. Mechanisms for counter- and co-current rotation drive are described and estimates of their magnitudes presented. A summary and discussion of open issues form the concluding section.

2. EXPERIMENTAL SUMMARY

Reduction of toroidal rotation by additional RF heating power in a predominantly NBI heated discharge appears to be a robust effect, which has been observed in a variety of operational regimes on different tokamaks.

On TFTR, this phenomenon was first observed in the deuterium beam heated L–mode discharges [15]. Figure 1 shows comparison of toroidal velocity profiles for the NBI heated discharges with and without additional RF heating power in both co- and counter-current dominated NBI cases. The toroidal velocity was measured by charge-exchange recombination spectroscopy (CER) utilizing the C VI 5292A transition line. The ICRF was tuned to the fundamental harmonic of H minority (Ω_H) and the second harmonic of D majority ($2\Omega_D$) near the magnetic axis. The companion shots had the same NBI parameters, similar pre-RF target plasma conditions and density evolution histories. The application of additional RF heating power caused substantial reduction of toroidal rotation in both co- and counter-injection analogous to momentum damping by viscosity. Small reduction of ion temperature was also observed in the process. In subsequent ICRF experiments on TFTR, similar RF rotation slowing phenomena were observed in supershot discharges using an on-axis ^{3}He minority heating scheme, in the direct electron heating regime, and in DT supershot using the Ω_H and $2\Omega_T$ heating schemes [3]. The effect appeared to be quite pervasive on TFTR, however, no reduction on toroidal rotation was seen in an off-axis D-^{4}He-^{3}He mode conversion heating experiment.

There were a number of reports on the effect of ICRF rotation slowing in NBI heated discharges from JET [4,16,17]. The ICRF heating scheme was of H-minority and phenomena observed were similar to those on TFTR.

On DIII–D, the fast wave (FW) power at high harmonics of ion cyclotron frequency is intended for electron heating and current drive. It was reported in the last RF
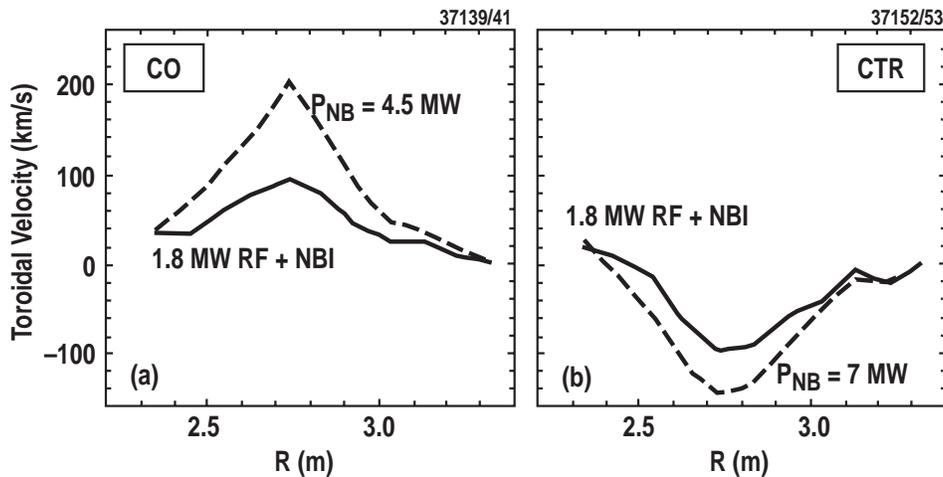
FIGURE 1. ICRF-reduction of V_{tor} first observed in TFTR L–mode plasmas.

conference [5] that addition of the FW power to NBI heated discharges also resulted in reduction of toroidal rotation as measured by CER. The effect to lowest order appeared to be independent of whether the antenna were phased for co- or counter-current drive. The magnitude of core toroidal rotation and the fractional reduction with FW are largest in the negative central magnetic shear (NCS) discharges which exhibit the internal transport barrier and have the core ion thermal diffusivity below the standard neoclassical value.

Smaller rotation reduction has also been observed in ELMing H–mode, high β_p H–mode, κ-ramped L–mode, and standard L–mode on DIII–D. Most interestingly, the phenomenon of RF rotation slowing was observed in recent DIII–D electron cyclotron heating (ECH) and current drive (ECCD) experiments (see Fig. 2) [18]. The effect occurred for ECH with radial and oblique launch, and was seen at varying levels with power deposition on-axis and off-axis. For all experiments to date on DIII–D the RF target discharge has its toroidal rotation first established with co-current NBI. It is of interest to see whether similar phenomena would be observed in counter-current NBI heated discharges on DIII–D

In the purely ICRF-heated discharges, counter-current toroidal rotation can be generated through a RF induced fast ion loss mechanism. This effect was most clearly demonstrated in a TFTR experiment [6]. The experiment was conducted using a series of discharges in which the H minority resonance layer was systematically moved outward from shot to shot by changing the magnetic field while keeping the edge q, plasma density, and RF power constant. The resonance surface was moved from $R = 2.70$ to 3.13 m which is at half of the minor radius. The plasma current was varied from 1.4 to 1.6 MA, central electron temperature from 3.0 to 4.0 keV, and electron density about 3×10^{19} m^{-3}. The applied ICRF power was 2 MW at 47 MHz with a symmetric wave spectrum. Plasma rotation was measured by the TFTR x–ray crystal spectrometer (XCS) system using the Doppler shifts of x–ray spectra of He-like iron, FeXXV. The key experimental result was that the magnitude of induced plasma rotation depends on the ICRF resonance location. In the case of the resonance surface located near the magnetic
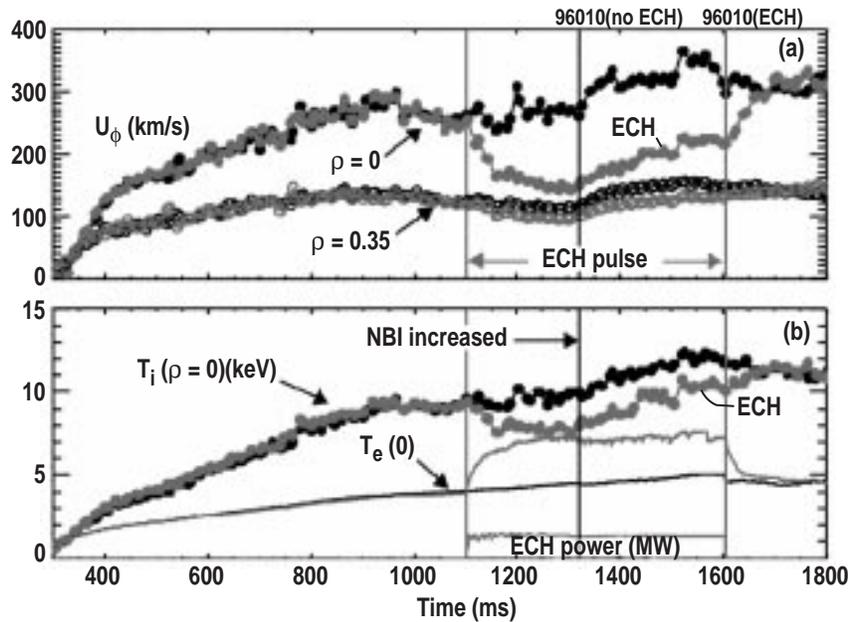
FIGURE 2. Electron heating with ECH also reduces NBI-driven rotation.

axis ($R = 2.70$ m), there was a barely noticeable toroidal rotation [see Fig. 3(a)]. When the resonance surface was moved off-axis ($R = 3.13$ m), the toroidal rotation reached a steady-state speed of about 50 km/s with the direction counter to the plasma current during the ICRF pulse [see Fig. 3(b)]. The induced poloidal rotation was not reported. There was also an anti-correlation between the measured toroidal velocity and the amount of the fast ion tail energy estimated from the diamagnetic and equilibrium measurements. This is consistent with the interpretation that the RF induced toroidal rotation is generated through a fast-ion loss mechanism. We note in passing that the counter-current rotation observed in the combined perpendicular NBI and ICRF heated discharges in JIPP TII-U [19] should share the same physical origin with that in this TFTR experiment, and is one of the earliest experiments to report ICRF acceleration of plasma rotation.
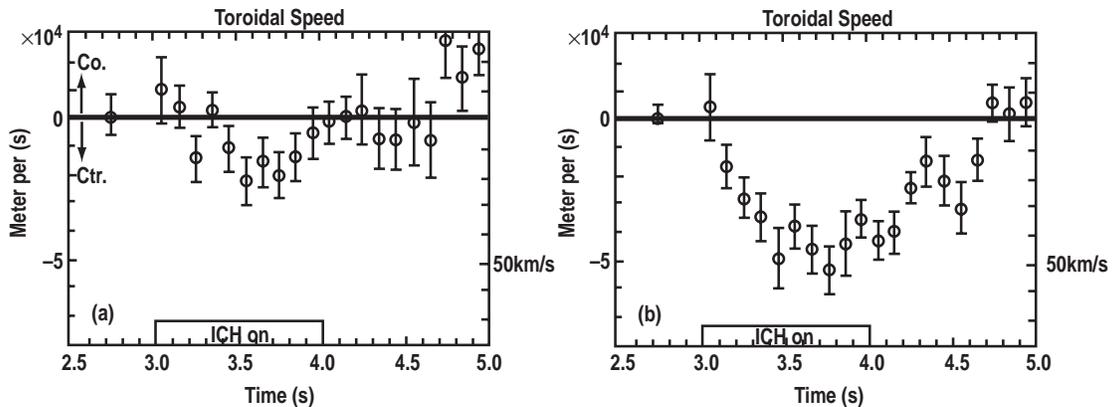
FIGURE 3. Counter toroidal rotation observed in ICRF-only TFTR discharges.

The RF induced co-current toroidal rotation has been observed in purely ICRF heated H–mode discharges in recent JET [7] and Alcator C-Mod [8] experiments. On both tokamaks, rotation was measured with XCS which utilized the spectrum of helium-like Ni^{+26} resonance line on JET and Ar^{+17} Lyman α doublet on C-Mod. ICRF was used in the H-minority heating regime and had a predominantly symmetric wave spectrum. Direct angular momentum input into the plasma was expected to be very small. In the JET experiments, substantial toroidal acceleration in the direction of the plasma current was observed at the transition into the H–mode. The rotation continued to increase throughout the RF phase, and never reached a saturation level. The maximum level measured corresponded to about 10%–20% of the rotation observed in the NBI heated discharges of similar experimental conditions. The increase of toroidal rotation was correlated with the increase of ion pressure gradient resulted from improved energy confinement in the H–mode. In the C-Mod experiments, the induced co-current toroidal rotation was observed also in conjunction with improved confinement, in particular with the onset of the H–mode (Fig. 4). However, significant core rotation observed cannot be accounted for by the increase of ion pressure gradient; a co-current core rotation with velocity up to 1.2×10^5 m/s, which corresponds to a main ion Mach number of 0.3, has been recorded. In general, the magnitude of observed rotation velocity increased with the stored energy increase, and the plasmas with highest H-factor rotated the fastest. For fixed stored energy increase, rotation velocity increased with decreasing plasma current, and reversed its direction when the plasma current was reversed. The radial profile of toroidal rotation velocity is peaked at the magnetic axis and falls off sharply with minor radius. The rotation appears to be more localized compared with that in the NBI heated discharges on other tokamaks. Inside the core region of the discharges, poloidal rotation is not measurable within experimental errors. The onset of the toroidal rotation and its decay after turn off the ICRF have similar time scales of 50–100 msec, which is slightly less than the energy confinement time, but still much longer than the momentum slowing down time predicted by the standard neoclassical theory.
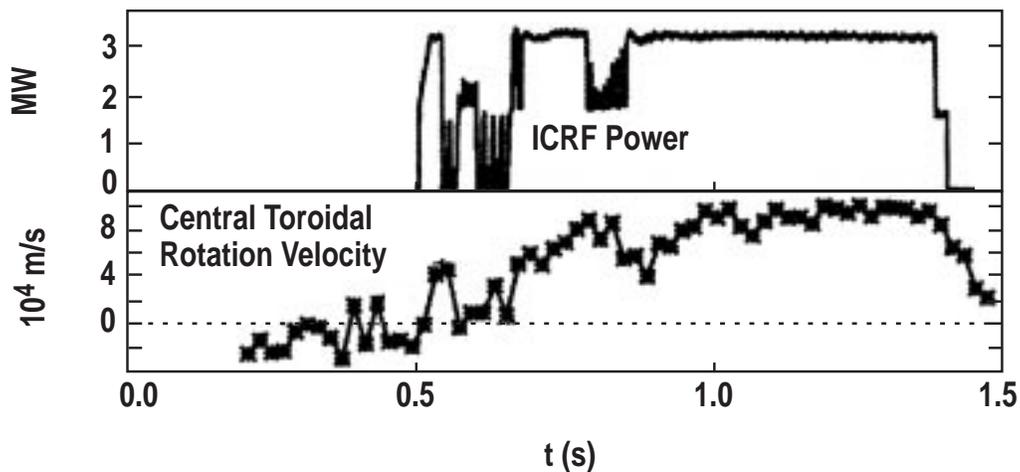
FIGURE 4. Significant co-current toroidal rotation observed in H–mode plasmas on C-Mod.

3. THEORETICAL MODELS

Our discussion of the theory for RF induced plasma rotation starts with a consideration of the toroidal and poloidal momentum equations. The toroidal momentum equation is [20]

$$m_i n_i \frac{d}{dt} \langle U_\phi R \rangle = -\frac{1}{c} \langle j_f \cdot \nabla \psi \rangle + \langle R \hat{e}_\phi \cdot F \rangle - \langle R \hat{e}_\phi \cdot (\nabla \cdot \Pi_I) \rangle \ , \tag{1}$$

Here, U is the flow velocity with the subscript ϕ indicating the toroidal direction, F is the frictional force acting on the electrons and ions by the fast ions, and $\langle j_p \cdot \nabla \psi \rangle \approx -\langle j_f \cdot \nabla \psi \rangle$ is used with j_p being the plasma current and j_f the fast ion current. The last term on the RHS is the toroidal component of the stress tensor and may be related to an empirical momentum confinement time τ_ϕ by setting

$$\langle \text{Re}_\phi \cdot (\nabla \cdot \Pi_I) \rangle \approx m_i n_i \frac{\langle U_\phi R \rangle}{\tau_\phi} \ . \tag{2}$$

Accordingly, the fast ion radial current provides an accelerating force, the frictional force can either accelerate (like in NBI) or decelerate the toroidal flow, and the stress tensor is a momentum sink carrying momentum away from the flux surface. In calculating the direction and magnitude of the toroidal rotation induced by any mechanism, all three terms have to be accounted for in general.

In deriving the poloidal flow velocity, incompressible constraint, *i.e.*, $\nabla \cdot U = 0$, is assumed, which to lowest order in gyroradius yields

$$U = K(\psi)B + G(\psi)R \hat{e}_\phi \ . \tag{3}$$

with the poloidal velocity $U_\theta = K(\psi)B_\theta$ and $G(\psi)$ is related to the perpendicular velocity on a flux surface. Using this expression for U in the parallel and poloidal momentum equations, the poloidal velocity is related to the parallel friction and rate of change of toroidal flow by

$$n_i K(\psi) \langle B^2 \rangle \approx \frac{\tau_i}{\varepsilon^{1/2}} m_i \left[\langle BF_\| \rangle - \frac{m_i n_i}{\langle R^2 \rangle} \frac{d}{dt} \langle U_\phi R \rangle \right] . \tag{4}$$

Note that Eq. (1) and Eq. (4) are coupled, hence any mechanism which drives toroidal flow will also drive poloidal flow. In particular, a fast ion radial current can produce a poloidal flow

$$K(\psi) = \frac{1}{m_i n_i c \, v_p} \frac{I}{\langle B_\theta^2 \rangle} \langle R^2 \rangle \langle j_f \cdot \nabla \psi \rangle \ , \tag{5}$$

with $v_p = \langle B^2 \rangle / \langle B_\theta^2 \rangle v_\|$, $v_\| \approx \varepsilon^{1/2} v_{ii}$, and ε being the inverse aspect ratio.

Various mechanisms can produce a fast ion radial current during ICRF heating. Because of neoclassical effect, trapped ions suffer collisions and diffuse outward resulting in a radially outward current. ICRF increases the energy of the trapped particles, further enhancing the fast ion diffusion and the fast ion radial current. In the case of confined fast ions, this does not necessarily drive plasma flow because the neoclassical effect produces a toroidally asymmetric fast ion velocity distribution whose frictional force on the bulk ions can exactly cancel the $j \times B$ torque created by the radial current, thus leaving the toroidal flow unchanged (see proof in Ref. 20). Nevertheless, the radial current can still drive a poloidal flow which is damped by the viscous stress.

The situation is different when the fast ions are not well-confined such as with the existence of a loss cone, produced for example by prompt orbit loss, large banana orbits hitting the limiter, or Alfvén eigenmodes which selectively eject energetic ions. Trapped fast ions which drift outward from the initial flux surface are lost for $r > r_0$ and lead to a counter-current torque on the bulk plasma. Although the fast ions distribution can still provide a frictional force opposing the torque, the two do not exactly cancel since the loss particles carry momentum out of the plasma. An estimate of the fast ion loss current may be obtained following [20] as

$$j_\mathrm{f} \approx e_\mathrm{f} \rho_{\mathrm{f}\theta} \varepsilon \frac{d}{dt} n_\mathrm{f} \ , \tag{6}$$

in steady-state and neglecting toroidal friction. Substituting Eq. (6) into Eq. (1) gives

$$U_\phi = -\mathrm{v}_\mathrm{f} \frac{m_\mathrm{f}}{m_\mathrm{i}} p_\mathrm{rf} \frac{\tau_\phi}{E_\mathrm{f}} n_\mathrm{i} \varepsilon \ , \tag{7}$$

with m_f, v_f, and E_f being the mass, characteristic velocity, and energy of the fast ions, m_i and n_i, the mass and density of the bulk ions, and p_rf is the power density. Taking $E_\mathrm{f} = 50$ keV, $p_\mathrm{rf} = 1$ W/cm^3, $n_\mathrm{i} = 2 \times 10^{14}$ cm^{-3}, and $\tau_\phi = 50$ ms, U_ϕ is approximately 30 km/s in the counter-current direction, which is a significant effect. The prediction is consistent with TFTR and JET results where slowing down of the toroidal rotation was observed when ICRF was added to co-current NBI. It is also consistent with counter-current NBI on JIPPT II-U but not TFTR.

In the case of purely ICRF minority or second harmonic heating using a symmetric antenna spectrum, the situation is similar and this mechanism always predicts a counter-current torque. For FW electron heating via Landau damping and transit-time magnetic pumping, or if ECH is applied, the reduction in toroidal rotation is possibly due to a reduction in the momentum confinement time τ_ϕ. Theory and simulation [21] have shown that reducing the ratio $T_\mathrm{i} / T_\mathrm{e}$ has a destabilizing effect on the ion temperature gradient turbulence thought to be responsible for the ion energy and particle confinement in tokamaks. If this also results in a degradation of momentum confinement, U_ϕ will decrease accordingly [see Eq. (7)].

While ICRF induced trapped particle loss is consistent with most of the off-axis heating experiments showing a reduction in rotation, it cannot explain the co-current

toroidal rotation observed in JET and Alcator C-Mod on-axis heating. A survey of the literature shows two theories [13,14], both invoking large drift-orbit physics, which predict a co-current rotation with ICRF heating of minority ions. Their arguments however are quite different.

The first theory [13] stresses that for the parameters in C-Mod, the ICRF interacts mainly with passing fast ions via the Doppler cyclotron resonance when the cold resonance is on-axis. Referring to Fig. 5, and focusing for the moment on a co-moving ($v_{\parallel} > 0$) passing ion, a $k_{\parallel} > 0$ wave can give a perpendicular kick to the ion at the low field resonance and causes the orbit to drift inward from its initial flux surface. By conservation of canonical momentum, it would return to its original position via a slightly smaller orbit if there is no further kick [Fig. 5(a)]. An identical ion at the high field resonance receives a kick from the $k_{\parallel} < 0$ wave and drifts outward from the flux surface returning to the original position via a slightly larger orbit [Fig. 5(b)]. If these two ions are one and the same, eventually the drift orbit will miss the high field resonance [Fig. 5(c)] and continues to spiral inwards due to the low field resonant interaction with the $k_{\parallel} > 0$ wave. The higher energy fast particles will be detuned from the high field resonance sooner (or if the plasma current is lowered), while at low enough energy, both resonances will stay active for a long time. The counter-moving ($v_{\parallel} < 0$) passing ion mirrors the behavior of the co-moving ion but at the high field resonance. The combined result is an inward drift of fast particle which produces a co-current toroidal torque on the bulk plasma. The Doppler resonance and toroidal effect work in concert to select a preferred drift direction and $k_{\parallel}$ sign.
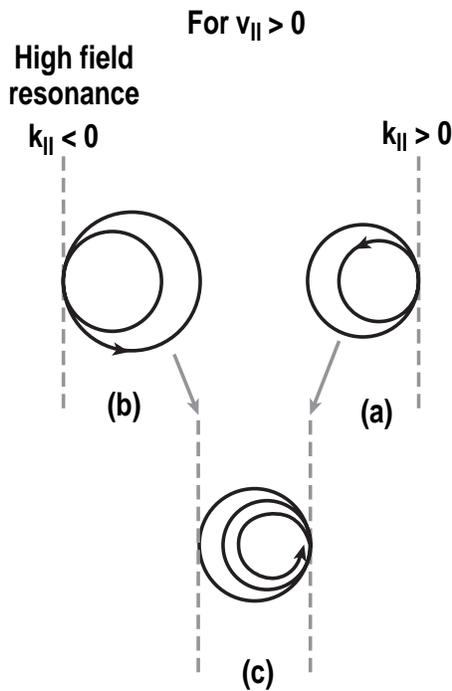
FIGURE 5. ICRF heating on energetic passing ions can produce inward drift.

In reality, a fast ion will encounter many collisions before achieving substantial orbit deviation, hence the inward drift can only be evaluated in a statistical sense. This was done in Ref. 13 using a guiding-center orbit code which includes a collision operator and an RF operator to model the perpendicular ''kick'' in velocity by the ICRF as the particle passes through a resonance. The calculation found that for C-Mod parameters, $j_f / e \approx - 0.3$ m/s, and substituting this in Eq. (1) assuming $\tau_\phi = 50$ ms and $n_i = 2 \times 10^{14}$ cm^{-3}, a toroidal rotation velocity in the co-current direction of the order of several tens of km/sec can be achieved, within the ball park of C-Mod experiment. Furthermore, the width of the rotation profile seems to correspond to the radius of the Doppler resonant layer for 50 keV particles, characteristic of fast ions produced by ICRF heating on C-Mod. We should point out that this estimate neglected the toroidal frictional force imparted by the fast ions on the bulk ions, which remains to be justified.

The theory of Ref. 13 produces a net toroidal torque on the bulk plasma. Even when the net torque is zero, large orbit effect can still produce a co-current rotation with ICRF minority heating [14]. To see that, consider the momentum diffusion equation in a cylinder (z is the symmetry axis),

$$\frac{d}{dt}\left(m_i n_i V_z\right) = \frac{1}{r}\frac{d}{dr}\left(\chi_M \frac{d}{dr} n_i m_i V_z\right) + F_z(r) \ , \tag{8}$$

where F_z is the axial force density and χ_M is the diffusivity for axial momentum density. In steady-state and applying the no-net-torque condition: $\int_0^a F_z(r) r\, dr = 0$ for $F_z(r)$ shown in Fig. 6,

$$n_i m_i V_z(r) = \int_r^{r_0} dr' \chi_M^{-1} \int_0^{r'} F_z(r'') r''\, dr'' \ , \tag{9}$$

where a no-slip boundary condition is also assumed. $V_z(r)$ from Eq. (9) has a co-current rotation profile extending from the axis to beyond the location of the axial force. An axial force with the prescribed profile can be produced by ICRF heating of trapped minority ions. During a poloidal circuit, a trapped ion can suffer a like-particle collision and take a step inward or outward depending on which orbit it is on. An ensemble of energetic trapped ions produced by ICRF heating will according to this mechanism generate side-by-side an inward and an outward fast ion radial current . The background plasma responds with equal and opposite currents which produce an axial torque with the sign and profile as indicating by F_z. By assuming that equal numbers of particles move in and out, and the half-width of the torque layer is given by the banana width: $\Delta r \approx (2 m_f E_f r_0 / R_0)^{1/2} / e B_\theta$, the toroidal velocity is estimated as

$$V_z(0) \approx p_{rf} \tau_\phi \frac{r_0 / R}{\pi e I_p \mu_0 R a^2 n_i} \ , \tag{10}$$
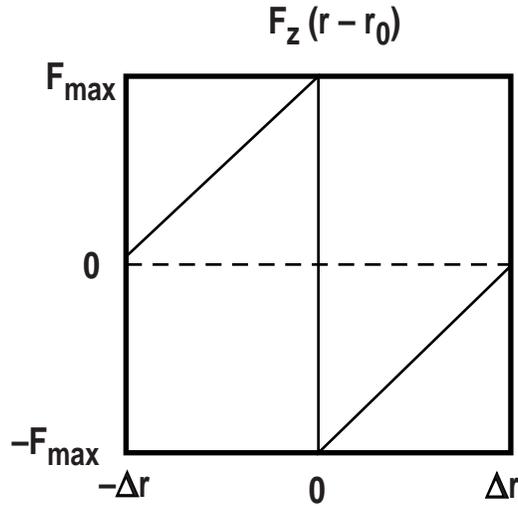
FIGURE 6. Profile of axial force density with no 'net'-torque.

with I_p being the plasma current. It increases with stored energy ($W \simeq p_{rf}\,\tau_\phi$) which is consistent with measurement. A key prediction is that, assuming the safety factor is close to one, the axial rotation by this mechanism scales as $T_i / B_\phi a$ or diamagnetically. Again, when Alcator C-Mod parameters are used, Eq. (10) yields an axial velocity between 30–100 km/s, qualitatively similar to the estimate obtained from the first theory although with quite different physics. More accurate calculation of the torque layer width using a guiding-center orbit code with the addition of the very important ion-ion collision physics should further refine the estimate.

4. CONCLUSION

This paper presents a brief review of the current understanding of RF-induced plasma rotation, both from experimental studies and theoretical investigations. It appears that reduction in toroidal rotation when ICRF is applied with and without NBI is consistent with RF induced loss minority ions. More study is needed to ascertain the existence of loss cones. With pure electron heating, momentum confinement degradation may be responsible for the smaller rotation. Momentum transport is not a well-understood topic and more experiments and theory in this area will be very beneficial.

The co-current rotation drive result is very intriguing and two promising theories have been proposed. Although the two theories give similar predictions, they can be distinguished by further experimental tests. For example, the first theory predicts the weakening of the effect as ICRF heating is moved off-axis, while the second theory in fact requires heating off-axis. The theory for treating large drift orbits is in its infancy and much more work lies ahead. The validity of the flux surface averaged momentum equations used to estimate the velocities, although well established in thin banana limit, may be called into question. Another challenge is accurately calculating the velocity

distributions for both the fast and background ions and ensuring that momentum conservation is obeyed in the collision and RF heating processes.

Finally, there are other novel ideas for RF induced rotation which are not discussed here for lack of space. These include non-resonant RF force (or ponderomotive drive) [22] and excitation of contained modes [23]. They may be relevant in some regime of the experimental parameter space but we should await for further theory development before passing judgment on these novel concepts.

ACKNOWLEDGMENT

REFERENCES

1. Strait, E.J., *et al.*, Phys. Rev. Lett. **74,** 2483 (1995).
2. Burrell, K.H., Phys. Plasmas **4,** 1499 (1997).
3. Phillips, C.K., *et al.*, APS (1997).
4. Stork, D., *et al.*, .Proc. 14th EPS Conf. on Contr. Fusion and Plasma Phys., Madrid, Vol.11D, I, 306 (1987).
5. deGrassie, J.S., *et al.*, Proc. 12th Top. Conf. on RF Power in Plasmas, Savanah, 93 (1997).
6. Husan, H., *et al.*, Proc. 11th Top. Conf. on RF Power in Plasmas, Palm Springs, p. 39 (1997).
7. Eriksson, L.G., *et al.*, Plasma Phys. Contr. Fusion **39**, 27 (1997).
8. Rice, J.E., *et al.*, Nucl. Fusion **38**, 75 (1998) .
9. LeBlanc, B.B., *et al.*, Phys. Plasmas **2**, 741 (1995).
10. Wilson, J.R., *et al.*, Phys. Plasmas **5**, 1721 (1998).
11. Chiu, S.C., *et al.*, Nucl. Fusion **29**, 1902 (1989).
12. Chan, V.S., *et al.*, Nucl Fusion **25**, 697 (1985).
13. Chang, S.C., Bull. Amer. Phys. Soc. **43**, No. 8, 173 (1998) H4I13.
14. Perkins, F.W., Bull. Amer. Phys. Soc. **44**, No. 1, Part II, 1265 (1999) RP01 123.
15. Jaehnig, K.P., *et al.*, APS (1988)
16. de Esch, H.P.L., *et al.*, Proc. 17th EPS Conf. on Contr. Fusion and Plasma Phys., Amsterdam, Vol.14B, I, 90 (1990).
17. O'Brien, D.P, *et al.*, Proc. 21st EPS Conf. on Contr. Fusion and Plasma Phys., Montpellier, Vol. 18B, I, 346 (1994).
18. deGrassie, J.S., *et al.*, Proc. 13th Top. Conf. on RF Power in Plasmas, Annapolis, 1999 (this conference).
19. Ida, K., *et al.*, Nucl. Fusion **31**, 943 (1991).
20. Rosenbluth, M.N., and Hinton, F.L., Nucl. Fusion **36**, 55 (1996).
21. Kinsey, J.E., General Atomics, private communication (1999).
22. Chan, V.S., *et al.*, Proc. Theory of Fusion Plasmas, Varenna, 1994, p. 89.
23. Coppi, B., *et al.*, Annals of Physics **261**, 117 (1997)